Journal of Catalysis **201,** 159–168 (2001)
doi:10.1006/jcat.2001.3256, available online at http://www.idealibrary.com on IDEAL®

Mechanism and Kinetics of the Selective NO Reduction over Co-ZSM-5 Studied by the SSITKA Technique

Part 1: NO_X Adsorbed Species Formation

E. M. Sadovskaya,* A. P. Suknev,* L. G. Pinaeva,* V. B. Goncharov,* B. S. Bal'zhinimaev,* C. Chupin,† and C. Mirodatos†,[1]

*Boreskov Institute of Catalysis, pr. Lavrentieva, 5, 630090, Novosibirsk, Russia; and †Institut de Recherches sur la Catalyse, 2 av. A. Einstein, F-69626 Villeurbanne Cedex, France

Received February 20, 2000; revised April 18, 2001; accepted April 19, 2001

A steady-state isotopic transient analysis of NO adsorption over Co-ZSM-5 catalyst in the absence or in the presence of oxygen is reported by using doubly labeled nitric oxide. The kinetics and mechanism of NO_X formation as well as the number of active sites for NO adsorption and their possible location on the catalyst surface are determined. The formation of $NO_2^{\delta+}$ species, active intermediates in deNO_X chemistry in the presence of oxygen and hydrocarbons, is shown to proceed according two sequential steps: (i) molecular oxygen adsorption and (ii) NO reaction with oxidized surface sites. The frequency factor of that reaction is found to be two orders of magnitude higher than that of mononitrosyls formation via the adsorption of NO on cobalt sites. The oxygen exchange within $NO_2^{\delta+}$ is considerably slower than the formation of that intermediate species, indicating that its two oxygen atoms are nonequivalent. The concentration of active sites leading to $NO_2^{\delta+}$ formation is also estimated and related to the interface existing between cobalt oxide clusters and zeolite framework.

Key Words: **SSITKA; kinetics and mechanism of NO adsorption; Co-ZSM-5 catalyst.**

INTRODUCTION

Selective catalytic reduction (SCR) of NO with CH_4 in the presence of excess oxygen over Co-ZSM-5 has been studied in recent years as a promising deNO_X technology. It is known that reaction rate increases substantially in the presence of O_2 (1–4), and that NO_2 can be easily formed in the excess of oxygen by the reaction of NO with O_2 (5, 6). Furthermore, the reaction of CH_4 with NO_2 proceeds with a comparable rate to that observed for $NO + O_2$ mixture (3, 4, 7, 8). Hence, in the oxidative atmosphere the reaction of NO reduction is thought to be initiated by the oxidation of NO to NO_2 followed by the interaction of CH_4 with either gaseous or adsorbed NO_2 (9–13).

However, despite intensive studies on reaction mechanism (4, 9–17), many features of the process remain unclear and controversial, particularly, the mechanism of formation of surface NO_X species responsible for methane activation. According to infrared data, the adsorption of NO over Co-ZSM-5 and Co-ferrierite leads to the formation of mono- and dinitrosyl complexes of cobalt on the catalyst surface in the absence of gaseous oxygen (10–12). In the presence of O_2, two additional bands appear in the spectrum; one of the bands at 1520 cm^{-1} can be assigned to nitrite–nitrate complexes and another band at 2130 cm^{-1} is usually related to $NO_2^{\delta+}$ species bound with acidic hydroxyl groups of zeolite (10–14, 18). Both nitrite (10–12) and nitrate (14) complexes were considered by different authors as possible candidates being responsible for the reaction with methane. Furthermore, participation of $NO_2^{\delta+}$ species in the SCR of NO_X over Cu-ZSM-5 (19) and H-ZSM-5 (20) was also proposed. Our previous DRIFT *in situ* study (17) showed that these species could be responsible for CH_4 activation because of their substantial decrease in concentration under reaction conditions as compared with that in $NO + O_2 + He$ mixture. However, both the mechanism of formation of $NO_2^{\delta+}$ species and their location on the surface is still widely discussed. Since these species were observed over a number of zeolite catalysts including H-form (11, 12, 17–22), they seem to be bound with hydroxyl groups and can be stabilized in metal-exchanged zeolites (12, 17, 19, 20). It was proposed in our previous paper (17) that $NO_2^{\delta+}$ species are located at the interface between cobalt clusters and zeolite lattice.

In this work, reported as Part 1, we focus on the formation of NO_X adsorbed species in the absence and in the presence of oxygen, but in the absence of methane, by using the Steady State Isotopic Transient Kinetic Analysis (SSITKA). Such a technique consists of analyzing the isotopic responses resulting from stepwise change

[1] To whom correspondence should be addressed. Fax:+33 4 72 44 53 99. E-mail: mirodato@catalyse.univ-lyon1.fr.

0021-9517/01 $35.00

of isotopic composition of the feed gas but maintaining an overall steady state of the catalysts, i.e., under adsorption/desorption/reaction equilibrium (23, 24). From this analysis the concentrations of different forms of adsorbed species as well as their formation rates can be evaluated, revealing the main elementary steps on the catalyst surface involving labeled molecules. Both the nitrogen and oxygen routes are investigated. In part Part 2, we will concentrate on the carbon routes which are related to the methane oxidation and determine the further key steps of NO_X reduction into N_2.

Under SSITK conditions, it should be noted that the dynamics of label transfer may include processes of isotopic exchange between adsorbed reacting intermediates and the bulk phases of the catalyst. Though rendering the interpretation of experimental results more complicated, these side isotopic transfers bring additional information on the state of the reacting adlayers under steady-state conditions. For the present case of NO activation, these two kinds of isotopic transfer phenomena can successfully be discriminated by using a molecule labeled in two positions, i.e., $^{15}N^{18}O$. The dynamics of nitrogen label (^{15}N) transfer should be determined only by catalytic processes since that element is only provided by the reacting feed and is not exchangeable with the bulk phases of the catalyst; in contrast, the oxygen label (^{18}O) may be controlled both by catalytic processes (with the same kinetic parameters as for the nitrogen label) and the isotopic exchange between reacting adspecies and the exchangeable pools of the catalyst (cobalt oxides and zeolite framework).

EXPERIMENTAL

The Co-ZSM-5 catalyst used in this study was prepared from H-ZSM-5 (SiO_2/Al_2O_3 ratio = 37) by ionic exchange technique with $Co(NO_3)_2$ solution followed by drying and calcining at 500°C. The cobalt content in Co-ZSM-5 was 1.8 wt% that corresponds to 1.9×10^{20} at.Co/g_{cat}. No bulk cobalt oxide phases (CoO or Co_3O_4) were detected by X-ray diffraction spectroscopy, indicating that the size of cobalt oxide clusters did not exceed 30–40 Å. Sieved 500–1000 μm particles were used in the present study.

The experiments were carried out by using a plug-flow reactor (ID = 3 mm, L = 120 mm) placed in a furnace. The catalyst was pretreated in 6% O_2 + He mixture at 500°C for one hour, then cooled to 450°C before admitting the NO + O_2 + He reacting mixture. When adsorptive equilibrium was achieved under $^{14}N^{16}O + O_2 + He$ flow, after about 8 minutes, gas flow was replaced stepwise by that containing $^{15}N^{18}O$ and vice versa. The isotope content was 94.6% of ^{15}N and 92.9% of ^{18}O for $^{15}N^{18}O$. In addition, this mixture also contained 0.2% of Ar as tracer to determine the mass-transfer regime degree of plug-flow approximation. From the shape of the step response of argon,

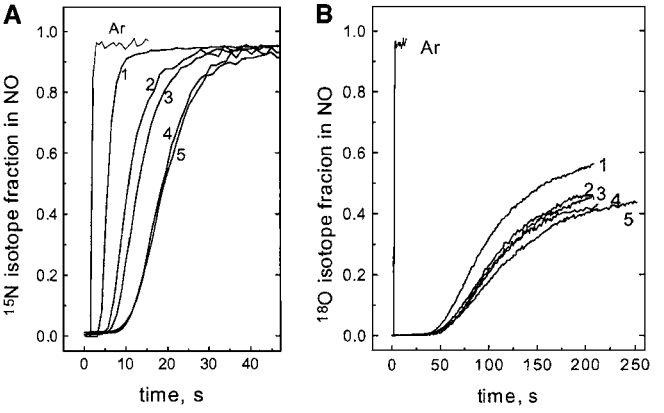

FIG. 1. Time dependencies of (A) ^{15}N and (B) ^{18}O isotopic fractions in NO compared to Ar response observed after $^{14}N^{16}O$ to $^{15}N^{18}O$ replacement in (1) NO + He flow and in NO + O_2 + He flows at (2) 0.15%, (3) 0.3%, (4) 1.5%, and (5) 3% oxygen content.

within one second, see Fig. 1, a CSTR behavior within gas scrambling in the catalyst bed can be excluded. The catalyst weight was equal to 0.22 g and gas flow rate –2 ml/s. The effluent gases from the reactor were continuously monitored by mass spectrometry. The concentrations of $^{14}N^{16}O$, $^{15}N^{16}O$, $^{15}N^{18}O$, $^{16}O^{18}O$, and $^{18}O^{18}O$ were determined from the intensities of parent peaks at m/e 30, 31, 33, 34, and 36, respectively. The peaks observed at m/e 46, 47, 48, 49, 50, and 51 were assigned to $^{14}N^{16}O_2$, $^{15}N^{16}O_2$, $^{14}N^{16}O^{18}O$, $^{15}N^{16}O^{18}O$, $^{14}N^{18}O_2$, and $^{15}N^{18}O_2$, respectively. The differentiation between $^{16}O_2$ and $^{14}N^{18}O$ (m/e = 32) was made considering that chemical gas concentrations were unchanged during isotopic transients.

The following isotopic experiments were performed:

1. Replacement of $^{14}N^{16}O$ by $^{15}N^{18}O$ in 0.6% NO + O_2 + He mixture. Concentration of O_2 was 0, 0.15, 0.3, 0.6, 1.5, and 3%.

2. Replacement of $^{14}N^{16}O$ by $^{15}N^{18}O$ in 1.2% NO + O_2 + He mixture. Oxygen concentration in these experiments was 0 and 3%.

RESULTS

1. $^{14}N^{16}O + He/^{15}N^{18}O + He$ Isotopic Switch

The changes of ^{15}N isotopic fraction in NO ($\alpha^{15}_{NO}(t)$) with time on stream after isotopic switch of NO in 0.6% NO + He flow was calculated as the sum of $^{15}N^{16}O$ and $^{15}N^{18}O$ concentrations divided by steady state NO concentration, i.e., the sum of $^{14}N^{16}O$, $^{15}N^{16}O$, $^{14}N^{18}O$, and $^{15}N^{18}O$ concentrations, as shown in Fig. 1A (curve 1). A delay of around 4 s is observed for ^{15}N appearance in the gas phase and the complete isotopic exchange of ^{14}N with ^{15}N in NO proceeds during the following 15 s. The amount of replaced nitrogen atoms calculated from the difference between the normalized Ar

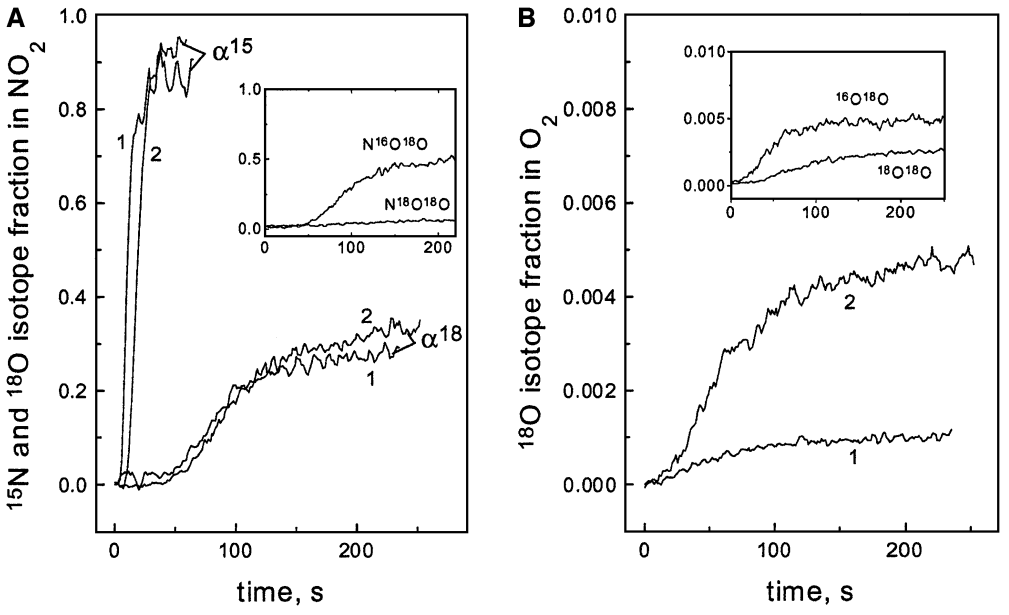

FIG. 2. Time dependencies of (A) ^{15}N and ^{18}O isotopic fractions in NO_2 and (B) ^{18}O isotopic fractions in O_2 observed after $^{14}N^{16}O$ to $^{15}N^{18}O$ replacement in (1) 0.6% NO + He and (2) 0.6% NO + 3% O_2 + He flows. Inserts: normalized concentrations of mixed and doubly labeled oxygen in (A) NO_2 and (B) O_2 observed after isotope replacement in 0.6% NO + 3% O_2 + He flow.

response and that of $\alpha^{18}_{NO}(t)$ is close to 0.06×10^{20} molec/g_{cat}. This pool of exchangeable N species value could arise both from adsorbed N-containing species and/or from the presence of gaseous NO accumulated in the zeolite pores. However, NO concentration in the pores cannot be larger than in the gas phase. Since catalyst pore volume was estimated to 0.5 cm^3/g_{cat}, the quantity of NO within the pores should not exceed the value of 0.0008×10^{20} molec/g_{cat}, which is negligible as compared to the above calculated pool. Therefore, the estimated amount of replaced nitrogen atoms should be mainly related to the N-containing adsorbed species. From the previously reported *in situ* IR study (17), these species must be ascribed to adsorbed NO species.

The delay for ^{18}O appearance is larger than that for ^{15}N (Fig. 1B, curve 1) indicating that there is a fast exchange between adsorbed NO species and the oxygen pools of the catalyst. However, unlike labeled nitrogen, the isotopic fraction of ^{18}O in NO ($\alpha^{18}_{NO}(t)$), calculated as the sum of $^{14}N^{18}O$ and $^{15}N^{18}O$ divided by steady-state NO concentration, does not reach rapidly a steady-state value but tails for a long time before stabilizing. This can be associated with a slow decrease of the rate of ^{18}O label transfer to the catalyst, as the maximum extent of catalyst oxygen isotopic exchange is raised.

2. $^{14}N^{16}O + {}^{16}O_2 + He / {}^{15}N^{18}O + {}^{16}O_2 + He$
Isotopic Switch

In the presence of oxygen, i.e., after replacing $^{14}N^{16}O$ by $^{15}N^{18}O$ in the 0.6% NO + O_2 + He flow, the shape of the $\alpha^{15}_{NO}(t)$ response is quite different than in the previously reported 0.6% NO + He flow (Fig. 1A, curves 2–5): (i) it is much more delayed and (ii) the complete nitrogen isotopic exchange is much more slowly achieved. ^{15}N label is also observed in NO_2 (Fig. 2A); however, the influence of this transfer on NO isotopic responses cannot be considered due to the very low NO_2 concentration (less than 0.5% from that of NO). One can therefore conclude that the response curve of ^{15}N obviously results from the superposition of two processes with distinct time constant. The first process corresponds to the fast isotopic exchange of the pool of reversibly adsorbed NO species, in a way similar as in the absence of oxygen. The second slower process indicates that there exists another pool of N-containing adspecies which exchanges more slowly with the gas phase. Changing oxygen concentration from 0.15 to 1.5% increases both the value of the delay and the input of the second species, so that the value of replaced nitrogen atoms is raised. However, increasing the O_2 content in the feed gas up to 3% does not change the shape of the response curve. The amount of exchangeable nitrogen atoms, estimated in the latter case, is found around 0.4×10^{20} atoms/g_{cat}.

The ^{18}O isotopic fraction in the same experiment is found to be lower than that observed in the absence of oxygen over the whole transient period (Fig. 1B, curves 2–5). This lower exchange can be due to a label transfer into new adsorbed O-containing ad- or gas species such as NO_2 and O_2 as well as to an increased rate of label transfer to the catalyst.

The ^{15}N isotopic fraction in NO_2 is increased in step with that in NO (Fig. 2A). Responses of ^{18}O isotopic fraction

are also similar to that in NO except for lower values of ^{18}O fraction in NO_2. In spite of high isotopic fraction of labeled oxygen in NO_2 reaching the value of $\alpha = 0.35$ after 200 s, $N^{18}O_2$ concentration remains close to zero within the whole studied transient period (Fig. 2A, insert). Note that if the oxygen label was statistically distributed in the labelled molecules, the fraction of $N^{18}O_2$ should have reached the value of $\alpha^2 = 0.12$. The absence of doubly oxygen labeled nitric dioxide means that one of the reaction intermediates directly participating in NO_2 formation do not contain labeled oxygen (or a negligible fraction). Hence, NO_2 formation would rather proceed via a mechanism which involves both the participation of labeled NO and unlabeled O_2.

The ^{18}O label appears in the gaseous oxygen earlier than in NO and NO_2 (Fig. 2B). The steady-state isotopic fraction in O_2 is reached rather rapidly after about 150 s after the isotopic switch. The fraction of labeled oxygen does not exceed 0.5% in all the experiments. The ^{18}O label can transfer into molecular oxygen after the decomposition of both gaseous NO_2 and NO_X adsorbed species. Such a low isotopic label concentration indicates that the rate of these two processes is low compared to that of the feed gas. One can see (Fig. 2B, insert) that the concentrations of mixed and doubly labeled oxygen increase simultaneously.

3. Simulation Results

As was noted above, the amount of labeled nitrogen atoms transferred into NO_2 does not exceed 0.5% from their total concentration in the feed gas. Obviously this transfer has a negligible influence on the ^{15}N label concentration in NO. Therefore, the dynamics of labeled nitrogen isotopic exchange are determined by the processes of NO adsorption and may be written according to usual mass balance equations,

$$\frac{\partial \alpha_{NO}^{15}}{\partial t} + \frac{U}{V}\frac{\partial \alpha_{NO}^{15}}{\partial \xi} = \frac{G}{VC_{NO}N}\sum_{i=1}^{n} W_i\left(\alpha_i^{15} - \alpha_{NO}^{15}\right)$$

$$\frac{\partial \alpha_i^{15}}{\partial t} = \frac{W_i}{\theta_i}\left(\alpha_{NO}^{15} - \alpha_i^{15}\right) \qquad [1]$$

Initial conditions $\quad t = 0: \quad \alpha_{NO}^{15} = 0, \quad \alpha_i^{15} = 0;$

Boundary conditions $\quad \xi = 0: \quad \alpha_{NO}^{15} = 0.95, \quad \alpha_i^{15} = 0;$

where α_{NO}^{15}, α_i^{15}- are the relative concentrations of ^{15}N isotopic label (isotopic fractions) in the gaseous NO and NO_X adsorbed species, respectively; C_{NO} is the concentration of NO in the gas phase (volume percent); θ_i is the concentrations of the ith adsorbed species on the catalyst surface [molec/g_{cat}]; W_i is the formation (decomposition) rate of adsorbed species [molec/g^*_{cat}s]; V is the reactor volume [cm^3]; U is the flow space velocity [cm^3/s]; G is the catalyst weight [g]; N is the Avogadro number; t is time [s]; ξ is the dimensionless bed length.

TABLE 1

Feed Gas Chemical Composition for Different Experiments

	Experiment number							
Concentration, %vol.	1a	1b	2a	2b	2c	2d	2e	2f
NO	0.6	1.2	0.6	0.6	0.6	0.6	0.6	1.2
O_2	—	—	0.15	0.3	0.6	1.5	3	3

The above system [1] is integrated over the whole bed length and transient period and the parameters fitted to the experimental data according to the elsewhere described procedure (25). The numerical analysis of isotopic responses $\alpha_{NO}^{15}(t)$ obtained in the absence of oxygen (Table 1, Exp. 1a and 1b) shows that adsorbed NO species are replaced with the same rate, i.e., that only one type of the surface complexes can be distinguished kinetically. In accordance with our previous DRIFT data in Ref. (17), these species are assigned to cobalt mononitrosyls, further denoted as [NO]. The values of mononitrosyl concentrations and their formation rates at different NO content are presented in Table 2.

The isotopic responses $\alpha_{NO}^{15}(t)$ obtained in the presence of O_2 can be considered as the superposition of the processes of NO adsorption–desorption on different adsorption sites. The fastest part of the relaxation curve, close to that observed in the absence of oxygen, can also be due to the isotopic exchange of cobalt mononitrosyls. In addition to the mononitrosyl adspecies, two [NO_X] species, formed in the presence of gaseous oxygen and differing by their isotopic exchange rate can be distinguished. According to the DRIFT data previously reported in (17), the [NO_X] species which are rapidly exchanged can be assigned to $NO_2^{\delta+}$ species, while the species much more slowly exchanged are assigned to stable nitrite complexes, denoted as [NO_2]. In contrast, much closer rates of exchange characterize the mononitrosyls and $NO_2^{\delta+}$ species. The nitrites concentration can therefore be determined independently, whereas there is a strong correlation between the concentrations of $NO_2^{\delta+}$ and mononitrosyls. Hence, in a first approximation the [NO] concentration was assumed not to change after oxygen addition, which allowed us to calculate the $NO_2^{\delta+}$ concentration. One can see (Table 2), that by increasing the gaseous oxygen concentration up to 1.5%, the surface coverage of $NO_2^{\delta+}$ species increased up to a limit value (corresponding to the total exchange capacity) substantially exceeding that of mononitrosyls species (e.g., for $NO:O_2 = 0.6:3.0$, [NO] = 0.64 and $[NO_2^{\delta+}] = 1.90$).

The rate of formation of [NO_X] adspecies was estimated within the framework of a simple parallel scheme: $NO \leftrightarrow [NO_X]_i$. As shown in Table 2, the rate of $[NO_2^{\delta+}]$ formation is always lower than that of [NO] but more than two orders of magnitude higher than that of [NO_2]. The comparison of calculated and experimental $\alpha_2^{\delta+}(t)$ responses for

TABLE 2

Estimated Values of [NO_X] Adsorbed Species Concentrations and Their Formation Rates

Gas phase concentration		Surface concentration			Rate of label transfer		
NO	O_2	[NO]	$[NO_2^{\delta+}]$	$[NO_2]$	[NO]	$[NO_2^{\delta+}]$	$[NO_2]$
C_{NO}	C_{O_2}	θ_1	θ_2	θ_3	W_1	W_2	W_3
[%vol]		[molec/g] × 10^{-19}			[molec/g*s] × 10^{-19}		
0.6	0	0.64	—	—	3.86	—	—
0.6	0.3	0.64	0.85	0.11	3.86	0.51	0.0016
0.6	0.6	0.64	1.05	0.15	3.86	0.73	0.0022
0.6	1.5	0.64	1.82	0.32	3.86	1.80	0.0048
0.6	3.0	0.64	1.90	0.53	3.86	1.85	0.0082
1.2	0	1.21	—	—	6.92	—	—
1.2	3.0	1.21	1.82	0.63	6.92	1.65	0.010

isotope experiments performed in 0.6% NO + He and 0.6% NO + 3% O_2 + He flows are presented in Fig. 3A.

The dynamics of ^{16}O replacement with ^{18}O in NO was considered to be determined by the following processes: (i) NO adsorption, (ii) oxygen exchange between different [NO_X] species and the catalyst oxygen pool, and (iii) partial oxygen transfer into NO_2 and O_2 due to the gaseous reaction: $2\,NO + O_2 \leftrightarrow 2\,NO_2$.

On the basis of our previous statements reported in (17), it is assumed that the oxygen atom of cobalt mononitrosyl can exchange directly only with the oxygen ions from the cobalt oxide clusters, whereas the oxygen atoms of $NO_2^{\delta+}$ species may exchange both with the cobalt oxide clusters and with the zeolite lattice. Since the [NO_2] formation rate was found to be extremely low, then it may be deduced that the NO ↔ [NO_2] ↔ [catalyst] transfer has a negligible influence on the observed rate of oxygen isotopic exchange in NO and can therefore be ignored. The reverse isotopic transfer from gaseous O_2 to NO, NO_2 and to the adsorbed layer can also be ignored because the ^{18}O isotopic fraction in O_2 never exceeded 0.005. Thus, the overall oxygen label transfer may be schematized as

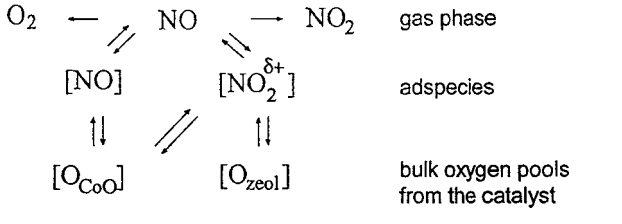

and the corresponding model for the ^{18}O label transfer can be written as

$$\frac{\partial \alpha_{NO}^{18}}{\partial t} + \frac{U}{V}\frac{\partial \alpha_{NO}^{18}}{\partial \xi} = \frac{G}{VC_{NO}N}\left(\sum_{i=1}^{2} W_i\left(\alpha_i^{18} - \alpha_{NO}^{18}\right) - (R_1 + R_2)\alpha_{NO}^{18}\right)$$

$$\frac{\partial \alpha_i^{15}}{\partial t} = \frac{W_i}{\theta_i}\left(\alpha_{NO}^{18} - \alpha_i^{18}\right) + \sum_{j=1}^{m}\beta_j\left(\alpha_j^{18} - \alpha_i^{18}\right)$$

$$\frac{\partial \alpha_j^{18}}{\partial t} = \sum_{i=1}^{2} m_i\beta_i\left(\alpha_i^{18} - \alpha_j^{18}\right) + \sum_{k=1}^{m} m_k\beta_k\left(\alpha_k^{18} - \alpha_j^{18}\right) \quad [2]$$

$$\frac{\partial \alpha_{O_2}^{18}}{\partial t} + \frac{U}{V}\frac{\partial \alpha_{O_2}^{18}}{\partial \xi} = \frac{G}{VC_{O_2}N} R_i \alpha_{NO}^{18}$$

$$\frac{\partial \alpha_{NO_2}^{18}}{\partial t} + \frac{U}{V}\frac{\partial \alpha_{NO_2}^{18}}{\partial \xi} = \frac{G}{VC_{NO_2}N} R_2 \alpha_{NO}^{18},$$

where α_{NO}^{18}, $\alpha_{O_2}^{18}$, $\alpha_{NO_2}^{18}$ are the ^{18}O isotopic fractions in NO, O_2, and NO_2, respectively; α_i^{18} and α_j^{18} are the ^{18}O isotopic fractions in [NO_X] surface species and in the catalyst (j indexes are related to different states of catalyst oxygen), respectively; m_{ij} and m_{jk} are the ratios between the amounts of exchangeable oxygen in ith surface species and jth oxygen states as well as between the different pools of catalyst oxygen, respectively; β_{ij} is the coefficient of isotopic exchange (s^{-1}); R_1 and R_2 are the rates of label transfer into O_2 and NO_2, respectively. The rates of NO ↔ [NO_X] transfer W_i and the concentrations θ_i were taken from the previous ^{15}N label transfer simulation.

Numerical analysis of isotopic responses obtained in the absence of oxygen showed that the exchange between the oxygen of the cobalt mononitrosyls and part of cobalt oxide oxygen proceeds more rapidly than NO adsorption, whereas the rate of label transfer into zeolite was considerably lower. Exchange coefficients and the amounts of exchangeable oxygen estimated within the above-proposed scheme are equal to

$$\beta_{[NO]-[CoO]} = 25\,s^{-1}, \quad \beta_{[CoO]-[ZEOL]} = 0.009\,s^{-1},$$

$$[O_{CoO}] = 1.4 \times 10^{20}\,at/g_{cat}, \quad [O_{ZEOL}] = 3 \times 10^{20}\,at/g_{cat}.$$

Figure 3B, shows that the difference between calculated and experimental responses obtained in 0.6% NO + He

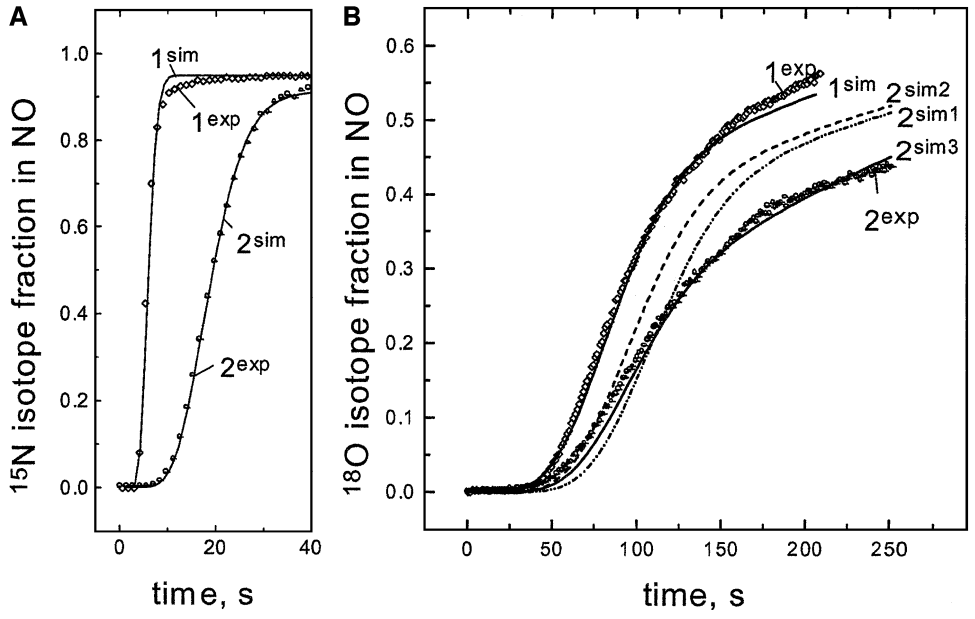

FIG. 3. Simulated (lines) and experimental (dotted) time dependencies of (A) ^{15}N and (B) ^{18}O isotopic fractions in NO observed after $^{14}N^{16}O$ to $^{15}N^{18}O$ replacement in (1) 0.6% NO + He and (2) 0.6% NO + 3% O_2 + He flows. Captions sim1, sim2, and sim3 correspond to simulated curves obtained by different simulation models (see text).

flow (curve 1) lies within the experimental error at these exchange coefficients values. Since the degree of ^{18}O exchange was limited to 60% in our experiments, only the fastest part of the exchange process could be analyzed. Hence, the calculated amount $[O_{ZEOL}]$ should be attributed to the oxygen species adjacent to or surrounding the oxide-like cobalt clusters rather than to the total amount of exchangeable zeolite oxygen. Hence the oxygen label transfer throughout the zeolite bulk is obviously controlled by slow diffusion processes.

In the presence of oxygen ($CO_2 > 1.5\%$) the rate of ^{18}O label transfer into the adsorbed layer is increased by about 1.5 times mainly due to the fast $[NO_2^{\delta+}]$ formation. This increase should result in a more prolonged delay for the ^{18}O appearance in the gaseous NO, as observed experimentally delay (Fig. 3B, curve 2). In addition, the time delay is also determined by the rate of homoexchange within $NO_2^{\delta+}$ species. Supposing a fast exchange, the calculated time delay is higher than the experimental delay (Fig. 3B, curve 2^{sim1}). Provided a low rate of homoexchange compared with that of $[NO_2^{\delta+}]$ formation and decomposition (Fig. 3B, curve 2^{sim2}), the initial parts of simulated and experimental responses coincide. However, it can be seen that the difference between the simulated and experimental $\alpha^{18}_{NO}(t)$ values increase with the degree of isotopic exchange. This discrepancy could be explain by the fact that $\alpha^{18}_{NO}(t)$ responses (Fig. 3B, curves 2^{sim1} and 2^{sim2}) are calculated without considering (i) the exchange between $NO_2^{\delta+}$ species and the catalyst oxygen pool or (ii) the partial ^{18}O label transfer into O_2 and NO_2. Taking into account the last process only, the calculated rate of the ^{18}O label transfer from NO to the catalyst bulk could be increased by the value of 5–7%. By considering also the direct exchange between $[NO_2^{\delta+}]$ and $[O_{ZEOL}]$ the calculated rate of label transfer into the catalyst bulk was also increased without shift of the initial part of the response (Fig. 3B, curve 2^{sim3}). The estimated values of oxygen exchange coefficients between $[NO_2^{\delta+}]$ and the catalyst are equal to

$$\beta_{[NO_2^{\delta+}]-[CoO]} \leq 0.05\ s^{-1}, \quad \beta_{[NO_2^{\delta+}]-[ZEOL]} = 0.031\ s^{-1}.$$

The above-proposed models (1) and (2) describe the time dependency of the isotopic fractions ^{15}N and ^{18}O, respectively, in the gas phase and in the adsorbed species, either in the absence or in the presence of oxygen. In the mean time, one can obtain additional information about the mechanism of label transfer into O_2 based on the isotopic distribution in O_2 (i.e., the ratio between the concentrations of doubly and singly labeled oxygen). It can be postulated *a priori* that the label transfer into O_2 results essentially from the decomposition of both gaseous NO_2 and adsorbed $[NO_X]$ species ($NO_2^{\delta+}$ and nitrite complexes) since it was checked that the direct O_2 exchange does not occur under the prevailing reaction conditions. The reaction of NO_2 decomposition is known to proceed via a bimolecular mechanism $2NO_2 \rightarrow 2NO + O_2$. Then, the ratio between doubly and singly labeled oxygen formed after NO_2 decomposition should obey a binomial distribution law

$$p = {}^{18}O^{18}O/{}^{18}O^{16}O = \alpha^2/2\alpha(1-\alpha),$$

where α is the ^{18}O isotopic fraction in NO_2.

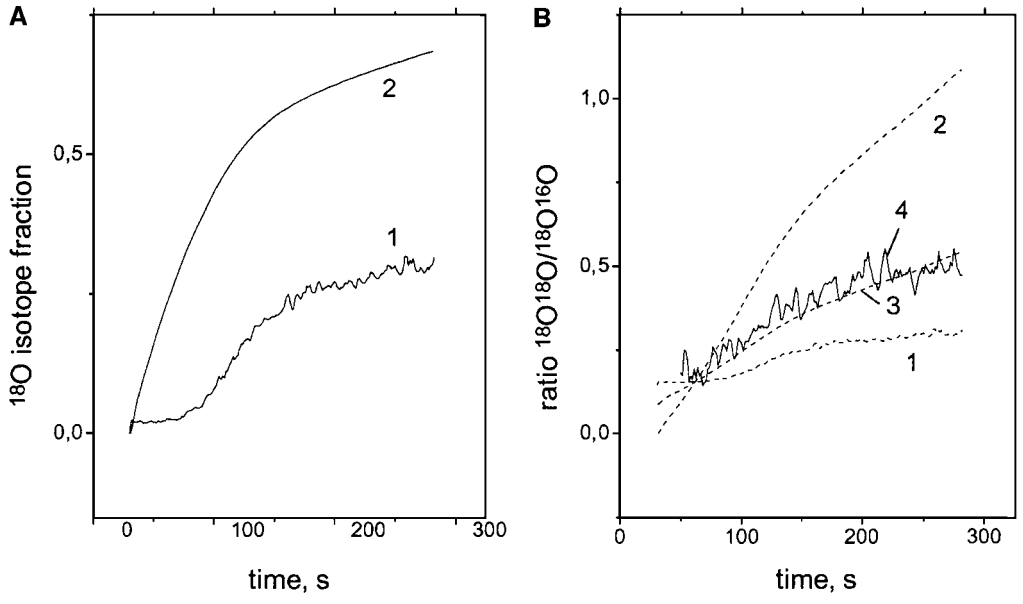

FIG. 4. (A) ^{18}O isotopic fractions in NO_2 (curve 1), in $[O_{CoO}]$ (curve 2) and in $[O_{ZEOL}]$ (curve 3) averaged along the catalyst bed; (B) ratio between $^{18}O_2$ and $^{16}O^{18}O$ (p(t)) calculated for ^{18}O label transfer from NO_2 (curve 1), from nitrite complexes (curve 2), and from $NO_2^{\delta+}$ species (curve 3) compared with the experimental (curve 4).

Figure 4 shows the time dependency of length-average $\alpha(t)$ values (Fig. 4A, curves 1–3) as well as calculated $p(t)$ dependency (Fig. 4B, curves 1–3) corresponding to these values. $\alpha(t)$ values were assumed to be equal to the half-sum of the isotopic fractions in NO_2 at the reactor inlet ($\alpha = 0.5$) and outlet. One can see that the calculated $p(t)$ dependency (Fig. 4B, curve 1) correlates well with the experimental dependency (Fig. 4B, curve 4), though, it lies some lower. As to the different variants of the label transfer from $[NO_X]$ species, the decomposition of $NO_2^{\delta+}$ species and nitrite complexes is thought to be accompanied by the formation of atomic oxygen [O] on the catalyst surface. In this case, $p(t)$ after oxygen desorption should also obey a binomial distribution law. It was supposed that the isotopic fraction in [O] is close to that in (a) the cobalt oxide after nitrites decomposition (Fig. 4A, curve 2) and (b) $[O_{ZEOL}]$ after $NO_2^{\delta+}$ decomposition (Fig. 4A, curve 3). The corresponding calculated $p(t)$ are presented in Fig. 4B, curves 2 and 3. As can be seen, the values and the characters of both calculated $p(t)$ dependencies are substantially different from the experimental dependencies. Hence, one can conclude that gaseous oxygen accepts ^{18}O label rather from NO_2 than from the catalyst surface. Taking into account all the processes of label transfer into O_2, the ratio between doubly and mixed labeled oxygen can be determined as

$$^{18}O^{18}O/^{18}O^{16}O = \Sigma w_1\alpha_i\alpha_i / \Sigma w_i 2\alpha_i(1-\alpha_i),$$

and the total amount of isotopic label in O_2 is equal to $NO = \Sigma w_I \alpha_i$.

Here, w_1 is the rate of NO_2 decomposition, w_2 and w_3 are the rates of oxygen desorption from the surface of oxide-like species and zeolite, α_i are the values of the isotopic fractions in NO_2, $[O_{CoO}]$ and $[O_{ZEOL}]$. The best simulation of the $p(t)$ curve was obtained with $w_1/w_2/w_3 = 6/2/1$ Absolute values of these rates can be determined on the basis of the total amount of labeled atoms in O_2. The rate of NO_2 decomposition was calculated to be 3.1×10^{16} molec O_2/s or 6.2×10^{16} molec NO_2/s per gram of the catalyst. The rates of oxygen desorption were estimated to be $w_2 = 1.2 \times 10^{16}$, $w_3 = 0.6 \times 10^{16}$ molec O_2/s per gram.

DISCUSSION

Within a zeolite catalyst, the dynamics of ^{15}N isotopic exchange during NO activation can be determined by a catalytic process (i.e., the rate of NO adsorption/desorption) as well as by a mass transfer process (i.e., the rate of NO diffusion in zeolite channels). If the rate of isotopic transfer was limited by NO diffusion, then the exchange rate of adsorbed NO species would depend on their location within the channels and the distance from the external catalyst surface. Accordingly, the ^{15}N isotopic responses should be determined by a *distribution of isotopic transfer rates* for each exchangeable components. However, the numerical analysis of isotopic responses obtained after switching from $^{14}N^{16}O$ to $^{15}N^{18}O$ in 0.6% NO + He and 1.2% NO + He flows revealed that the adsorbed mononitrosyl complexes can be characterized by a single exchange rate. Hence, the rate of diffusion is thought to be

larger than the rate of cobalt mononitrosyls formation and decomposition, which rules out any mass transfer diffusion control.

In the presence of oxygen, a significant delay is observed in the isotopic transient curves, which could also be related to NO mass transfer limitation, oxygen possibly hindering the internal diffusion of NO molecules. In that case, the rate of mononitrosyls isotopic exchange should decrease significantly, which was *not* revealed by the numerical analysis of the transient curves. Therefore the rate of NO internal diffusion is thought to remain high in the presence of oxygen and still not interfering with the isotopic transfer dynamics. Accordingly, the existence of both quickly and slowly exchangeable components revealed by the analysis of the isotopic responses do result from the convoluted formation and decomposition rates of distinct adsorbed $[NO_X]$ species. Based on the obtained estimations of $[NO_X]$ species concentrations and their decomposition rates (Table 2), their average lifetime may straightforwardly be estimated (23, 24). Cobalt mononitrosyls, $NO_2^{\delta+}$ species, and nitrite complexes have an average lifetime of about 0.16, 1, and 100 s, respectively. This ranks unambiguously their relative stability, in perfect agreement with the direct DRIFT observations (17).

The concentration of mononitrosyls is proportional to the NO content in the feed gas indicating that the steady-state surface coverage of these species is far from saturation, and thus most of the cobalt active sites remain unoccupied in the range of NO and O_2 concentrations used in this study (see Experimental). In contrast, the coverage of $NO_2^{\delta+}$ species approaches the maximum value within the same concentration range. This means that only part of the cobalt active sites participate in $NO_2^{\delta+}$ formation.

As above mentioned, the responses of ^{18}O isotopic fraction in NO arise from the superposition of both fast and slow processes. The fast processes correspond to the isotopic exchange of oxygen atoms belonging to NO_X adspecies and to the exchange with surface oxygen directly bound to the adsorption sites, as revealed as the increased delay of the ^{18}O label appearance compared to that of ^{15}N. The slow process most likely corresponds to the exchange of oxygen from the zeolite lattice. From the numerical analysis, the amount of quickly replaced oxygen was found to be about 1.4×10^{20} at/g_{cat}, that corresponds to 70% of the total amount of oxygen atoms contained in the CoO cobalt clusters (2.0×10^{20}). Since, as mentioned by Li and Armor (26), each isolated cobalt ion (Co^{2+}) is able to adsorb NO, the above value corresponds to the actual dispersion of the cobalt atoms within the zeolite and confirms the existence of micro clusters in our catalytic system.

The number of active sites can also be estimated by comparing the transient isotopic experiments with the DRIFT data (17). According to the DRIFT data, the concentration of cobalt mononitrosyls was decreased by about 25% after oxygen addition into NO + He flow. This decrease was assumed to arise from the occupancy of part of the cobalt active sites by $NO_2^{\delta+}$ species, preferentially, and by nitrite complexes. Considering a first-order adsorption mode, the concentration of cobalt mononitrosyls θ_1 should be proportional to the number of unoccupied active sites $\theta_1 = K_R C_{NO}(L - \Sigma\theta_i)$, where K_R is the equilibrium constant, L is the total number of active sites, and the concentration of unoccupied active sites can be written as

$$L - \theta_1 = (\theta_2 + \theta_3)/0.25.$$

In experiments performed with the same NO and O_2 content, the total concentration of $NO_2^{\delta+}$ species and nitrite complexes $(\theta_2 + \theta_3)$ was found to be about 3×10^{19} molec/g_{cat}. Since the mononitrosyl concentration is proportional to that of NO, then $L \gg \theta_1$. The quantity of these sites L is estimated to be $3 \times 10^{19}/0.25 = 1.2 \times 10^{20}$ sites/g_{cat}. This value is in excellent agreement with the value of accessible Co atoms previously determined from NO adsorption in the absence of oxygen (1.4×10^{20} at/g_{cat}), within the accuracy of our estimations (about 10%).

The formation of $NO_2^{\delta+}$ species was proposed in Ref. (17) to involve both zeolite hydroxyl groups and cobalt oxide clusters. The observation in the present paper that (i) the rate of the ^{18}O exchange between $NO_2^{\delta+}$ and cobalt oxide is considerably lower than that for mononitrosyls, and (ii) there exists a slow but significant oxygen exchange between $NO_2^{\delta+}$ and the zeolite strongly confirms the interfacial location of the $NO_2^{\delta+}$ species. Thus, the maximum value of $NO_2^{\delta+}$ concentration is determined by the number of boundary active sites, which is equal to 2×10^{19} sites/g_{cat}, i.e., 10% of the total number of cobalt atoms.

As revealed by the low label concentration in gaseous O_2, the rate of ^{18}O label transfer from NO to molecular oxygen was found to be extremely low. Our calculations confirm that the rate of $NO_2^{\delta+}$ decomposition is more than two orders of magnitude higher than that of the label transfer from the adsorbed layer to the gaseous oxygen (see Simulation results). One can conclude that there is a slow step in $NO_2^{\delta+}$ formation, which is most likely related to the modification of active sites under the action of oxygen. This step should be reversible and determined by the low rate of dissociative oxygen adsorption, which also proceeds at the interface between cobalt oxide clusters and zeolite.

On the basis of the above estimations of coverages and numbers of active sites, the rate constants of formation/decomposition processes for both mononitrosyls and $NO_2^{\delta+}$ species can be determined. Considering that the formation of mononitrosyls Co(NO) results from the direct interaction of NO with free active sites of cobalt oxide [*],

the corresponding first-order kinetic equations can be written as

$$NO + [^*] \leftrightarrow [NO] \quad W_1 = k_1 C_{NO} \theta_{[^*]}, \quad W_{-1} = k_{-1}\theta_1, \quad [3]$$

where W_i and W_{-i} are the rates of forward and backward steps [molec./g_{cat} s], k_1 and k_{-1} are the corresponding rate constants [s^{-1}], C_{NO} is the concentration of NO in the gas phase [% vol.], $\theta_{[^*]}$ and θ_1 are the concentrations of free active sites and cobalt mononitrosyls [molec/g], respectively. In the absence of O_2, NO is adsorbed only as cobalt mononitrosyls, and $\theta_{[*]} = L - \theta_1$ with $L = 1.4 \times 10^{20}$ total number of active sites, as above determined. Then, the rate constants

$$k_1 = \frac{W}{C^*_{NO}(L - \theta_1)}, \quad k_{-1} = \frac{W_{-1}}{\theta_1},$$

can be straightforwardly be deduced from the data of Table 2 as

$$k_1 = 48(\pm 5)\ s^{-1}, \quad k_{-1} = 6(\pm 1)\ s^{-1}.$$

As shown above, the formation of $NO_2^{\delta+}$ species proceeds sequentially by the step of oxygen adsorption at the boundary of cobalt oxide and zeolite (kinetics of this step cannot be determined from the obtained results), followed by NO adsorption on oxidized active sites

$$[O] + NO \leftrightarrow [NO_2^{\delta+}] \; W_2 = k_2 C_{NO} \theta_{[O]}, \; W_{-2} = k_{-2}\theta_2, \quad [4]$$

where θ_2 and $\theta_{[O]}$ are the concentrations of $NO_2^{\delta+}$ species and oxidized sites, respectively. Since an increase of NO content from 0.6 to 1.2% does not change $NO_2^{\delta+}$ concentration, this means that the equilibrium of step 2 is strongly shifted to the right under these conditions; it may then be assumed reasonably that the concentration of oxidized sites [O] does not exceed 5% from that of θ_2. Therefore,

$$k_2 \geq \frac{W_2}{C_{NO} 0.05^* \theta_2} = 3300\ s^{-1},$$

$$k_{-2} = \frac{W_{-2}}{\theta_2} = 0.8(\pm 0.2)\ s^{-1},$$

The ratio k_1/k_2 between the adsorption rate constants for reactions [3] and [4] gives straightforwardly the ratio between the frequency factors for these two reactions. It comes that NO is activated into $NO_2^{\delta+}$ with a probability about two orders of magnitude higher than for NO activation into cobalt mononitrosyls.

As to nitrite complexes, the rate of their decomposition (formation) is somewhat lower than that of the label transfer into the gaseous oxygen. However, the rate of label transfer into O_2 is determined by the decomposition rate of both NO_X adsorbed species and gaseous NO_2. Though no definite mechanism of nitrite formation/decomposition can be derived from this study, these species presumably originate from the interaction of both mononitrosyls with molecular oxygen and adsorbed oxygen with NO. In addition, the rate of their formation is comparable to that of gaseous NO_2 formation (see Simulation results). Thus, NO_2 adsorption can also contribute significantly to the rate of nitrite formation.

CONCLUSION

The present SSITKA study of NO adsorption by using doubly labeled nitric oxide allowed us to draw advanced conclusions on the kinetics and mechanism of NO_X formation as well as to estimate the number of active sites for NO adsorption and their possible location on the catalyst surface. The rate of gaseous NO_2 formation was found to be comparable with that of nitrite formation and substantially lower than that of $NO_2^{\delta+}$ formation. Therefore $NO_2^{\delta+}$ species cannot originate from NO_2 adsorption but are formed in two sequential steps: (i) molecular oxygen adsorption and (ii) NO reaction with the oxidized surface sites. Step (ii) is highly favored even at small NO content, which results in a very low concentration of free oxidized sites. Thus the frequency factor of that reaction is found to be two orders of magnitude higher than that of mononitrosyls formation via the adsorption of NO on cobalt sites. The rate of oxygen exchange within $NO_2^{\delta+}$ is considerably lower than that of their formation indicating that the two oxygen atoms of that intermediate species are nonequivalent. The concentration of active sites leading to $NO_2^{\delta+}$ formation was also estimated and related to the interface existing between the cobalt oxide clusters and zeolite phases.

ACKNOWLEDGMENTS

This work was carried out within the Twinning Program between Boreskov Institute of Catalysis (Novosibirsk) and Institut de Recherches sur la Catalyse (Lyon). The research was partially supported by Russian Fund of Basic Research, Grant 00-03-22004.

REFERENCES

1. Vassallo, J., Miro, E., and Petunchi, J., *Appl. Catal. B* **7**, 65 (1995).
2. Burch, R., and Scire, S., *Appl. Catal. B* **3**, 295 (1994).
3. Li, Y., and Armor, J. N., *Appl. Catal. B* **2**, 239 (1993).
4. Witzel, F., Sill, G. A., and Hall, W. K., *J. Catal.* **149**, 229 (1994).
5. Petunchi, J. O., and Hall, W. K., *Appl. Catal. B* **2**, L17 (1993).
6. Shelef, M., Montreuil, C. N., and Jen, H. W., *Catal. Lett.* **26**, 277 (1994).
7. Lukyanov, D. B., d'Itri, J. L., Sill, G., and Hall, W.K., *in* "11th Int. Cong. Cat.—40th Anniv.," Vol. 101, p. 651, 1996.
8. Li, Y., and Armor, J. N., *J. Catal.* **150**, 376 (1994).
9. Cowan, A. D., Dumpelmann, R., and Cant, N. W., *J. Catal.* **151**, 356 (1995).

10. Li, Y., Slager, T. L., and Armor, J. N., *J. Catal.* **150**, 388 (1994).
11. Bell, A. T., *Catal. Today* **38**, 151 (1997).
12. Aylor, A. W., Lobree, L. J., Reimer, J. A., and Bell, A. T., *in* "11th Int. Cong. Cat.—40th Anniv.," Vol. 101, p. 661, 1996.
13. Adelman, B. J., Beutel, T., Lei, G.-D., and Sachtler, W. M. H., *J. Catal.* **158**, 327 (1996).
14. Sadykov, V. A., Beloshapkin, S. A., Paukshtis, E. A., Alikina, G. M., Kochubei, D. I., Degtyarev, S. P., Bulgakov, N. N., Veniaminov, S. A., Netyaga, E. V., Bunina, E. V., Kharlanov, A. N., Lunina, E. V., Lunin, V. V., Matyshak, V. A., and Rozovskii, A. Ya., *Polish J. Environ. Studies* **6**, 21 (1997).
15. Cowan, A. D., Cant, N. W., Haynes, B. S., and Nelson, P. F., *J. Catal.* **176**, 329 (1998).
16. Lombardo, E. A., Sill, G. A., d'Itri, J. L., and Hall, W. K., *J. Catal.* **173**, 440 (1998).
17. Pinaeva, L. G., Sadovskaya, E. M., Suknev, A. P., Goncharov, V. B., Sadykov, V. A., Balzhinimaev, B. S., Decamp, T., and Mirodatos, C., *Chem. Eng. Sci.* **54**, 4327 (1999).
18. Hoost, T. E., Laframboise, K. A., and Otto, K., *Catal. Lett.* **33**, 105 (1995).
19. Valyon, J., and Hall, W. K., *J. Phys. Chem.* **97**, 1204 (1993).
20. Hadjiivanov, K., Saussey, J., Freysz, J. L., and Lavalley, J. C., *Catal. Lett.* **52**, 103 (1998).
21. Iwamoto, M., Hidenori, Y., Mizuno, N., Zhang, W.-X., Mine, Y., Furukawa, H., and Kagawa, S., *J. Phys. Chem.* **96**, 9360 (1992).
22. Beutel, T., Adelman, B. J., and Sachtler, W. M. H., *Appl. Catal. B* **9**, L1 (1996).
23. Happel, J., "Isotopic Assessment of Heterogeneous Catalysis." Academic Press, New York, 1986.
24. Mirodatos, C., *Catal. Today* **9**, 83 (1991).
25. Sadovskaya, E. M., Bulushev, D. A., and Bal'zhinimaev, B. S., *Kinet. Katal.* **40**, 61 (1999).
26. Li, Y., and Armor, J. N., *Appl. Catal. B* **2**, 239 (1993).